



# Hypothesis-driven analysis of a 19-color deep immunophenotyping panel using automatic gating

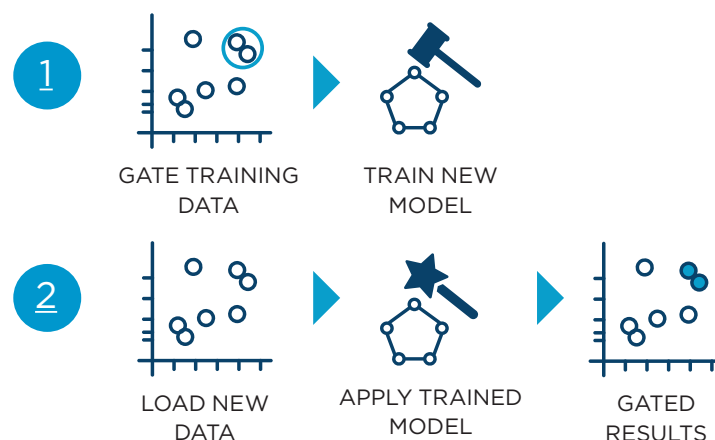
## Objective

- Understand an exemplary deep immunophenotyping panel appropriate for the CytoFLEX LX flow cytometer
- Compare the results of manual and automatic hypothesis-driven analysis
- See the reduction in hands-on time when using Cytobank Automatic gating

Immunophenotyping is widely used to identify perturbations of the immune system due to disease conditions or therapeutic or protective interventions in the study of infectious diseases and vaccination, cell and gene therapy or basic research into the function of the immune system. Deep immunophenotyping refers to the use of high-dimensional cytometry using marker panels covering a high number of markers, allowing the identification of cellular subsets of multiple lineages and deep hierarchies.

Deep immunophenotyping results in complex data that can be challenging to analyze by manual gating alone. For the discovery of disease-specific molecular signatures and disease-associated phenotypes, even with an incomplete understanding of pathophysiological mechanisms, unsupervised machine learning algorithms provide significant advantages over manual gating. However, they often do not allow the identification of previously described populations according to user-defined criteria. In this hypothesis-driven setting, the automation of classical gating approaches can increase the reproducibility and decrease hands-on time.

In this whitepaper, we demonstrate how Cytobank Automatic gating can be used to faithfully replicate manual gating steps for the identification of cellular subsets. In addition, we show that Cytobank Automatic gating reduces hands-on time required for the analysis of high-dimensional cytometry data.



## A deep immunophenotyping panel identifies 44 distinctive cell populations

A 19-color staining panel was developed to stain whole blood samples using DURAClone IM T-cell Subsets dry reagent for backbone markers and drop-in liquid antibodies as well as a fixable viability dye (FVD), ViaKrome 808. Whole blood samples were stained and analyzed on a Beckman Coulter Life Sciences CytoFLEX LX flow cytometer with WDM Beam Splitter. S/N BC19201 using a U3-V5-B3-Y5-R3-I2 detector configuration with the standard filter set (PN: C42428 Rev AA, CytExpert, version 2.4).

	375 nm			405 nm					488 nm		561 nm				633 nm		808 nm		
Channel	405/30	525/40	675/30	420/45	525/40	610/20	660/10	763/43	525/40	690/50	585/42	610/20	675/30	710/50	763/43	660/10	712/25	763/43	885/40
Specificity	CD15	CD16	HLA-DR	CD57	CD45	CD19	CD14	CD20	CD45RA	CD56	CCR7	CD28	CD33	PD-1	CD27	CD4	CD8	CD3	L/D
Fluorophore	BUV 395	BUV496	BUV661	Pac Blue	KrO	BV 605	BV 650	BV 785	FITC	BB700	PE	ECD	PC5	PC5.5	PC7	APC	AF700	APC AF750	Viability 808

For the hypothesis-driven definition of leukocyte and lymphocyte subsets, 25 gates were defined and combined using a Boolean AND operator to identify 44 populations (**Figure 1**). Gate positions were tailored by file. Ten samples were used to train an automatic gating model. The trained model was used to run inference on the remaining 10 samples. For a detailed description of the workflow, see the *How to establish and evaluate machine learning-assisted automatic gating to improve reproducibility and reduce time spent for your flow cytometry data analysis* application note.

On the Cytobank platform, a gate is defined as a shape drawn on a plot to encapsulate a set of events, but other than that, it carries no other information about hierarchy or complex cellular identity. Populations are defined by a collection of gates including information about hierarchy to categorize cellular identity.

Cleanup gating was performed to exclude doublets, dead cells and debris, identifying viable CD45+ leukocytes. An overview of all identified populations is provided in the population tree and a sunburst plot for a representative sample:

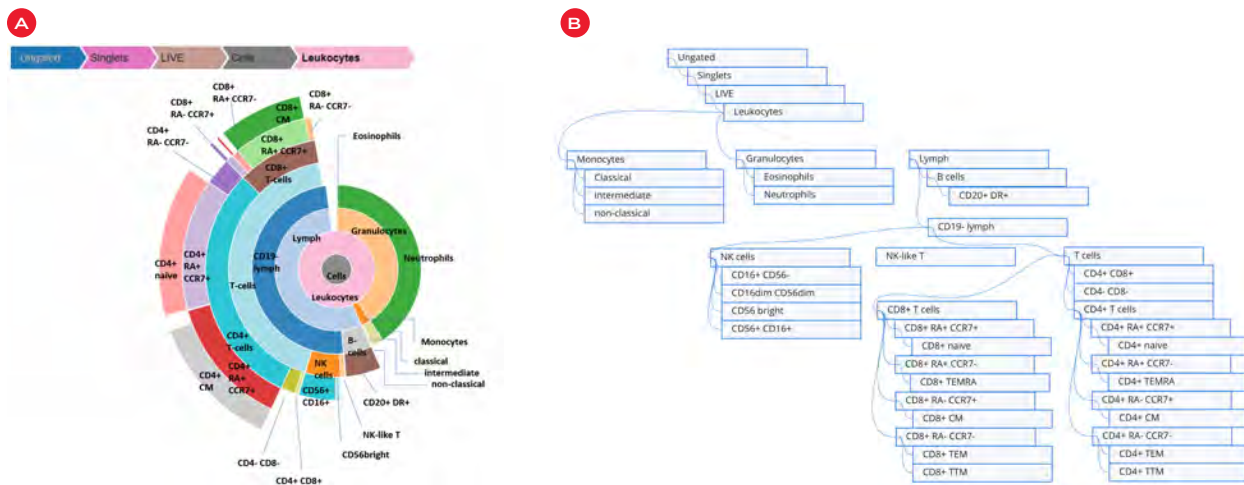


**Figure 1.** (A) Sunburst plot of one experimental file showing population distribution. (B) Population hierarchy of all 44 populations.

## Automatic gating faithfully reproduces manual gating results

Manual gating is considered to be a significant source of variability for flow cytometry assays. Automatic approaches can reduce the intra-operator variability and fully remove inter-operator variability when trained models are shared between users. Here we show that Cytobank Automatic gating can reproduce manual gating results for different types of manually identified populations.

An automatic gating model was trained on 5 samples stained and acquired on day one and 5 samples stained and acquired on day two on the Cytobank platform. The model was applied to the remaining 10 samples and results compared against manual gating results.

Shown are 5 representative populations, covering a variety of use cases.

### Cells population: polygonal gate on heterogeneous scatter population

The Cells population was identified as part of cleanup gating.

#### Cells

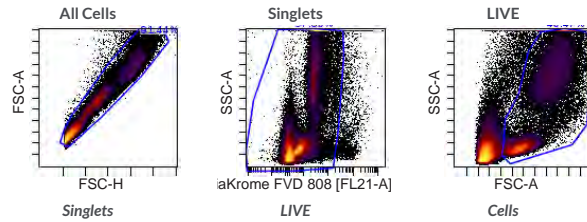


Figure 2. Gating hierarchy of Cells population.

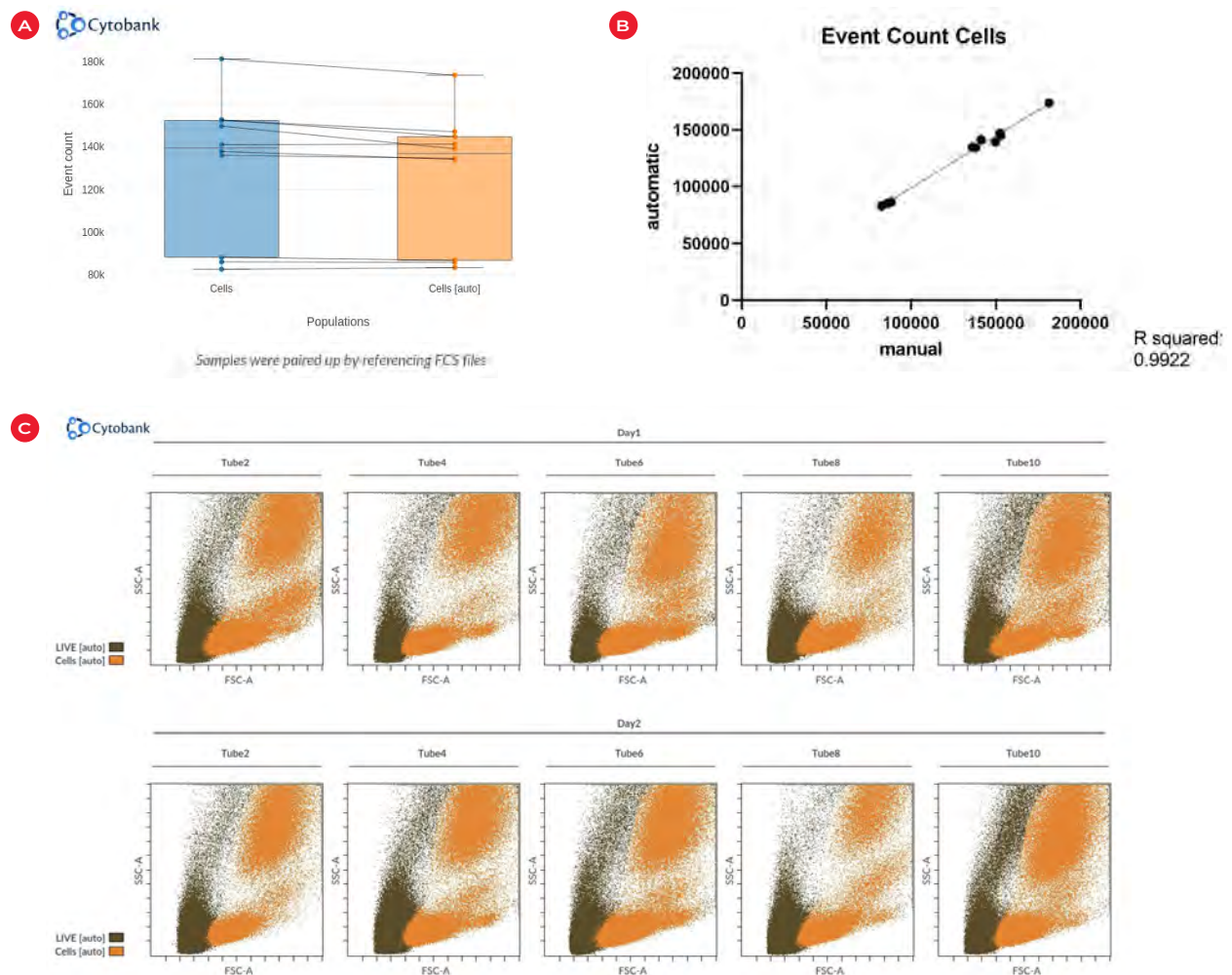


Figure 3. (A) Box plot comparing event count of manually and automatically gated Cells population. (B) Correlation of manual and automatic Cells population. (C) Dot plots for 5 exemplary samples with automatically identified LIVE and Cells populations in the overlaid position.

## B cells: distinct population using split gate

B cells were identified based on their CD45 expression, absence of CD33 expression to exclude monocyte contamination from the lymphocyte population and CD19 positivity.

### B cells

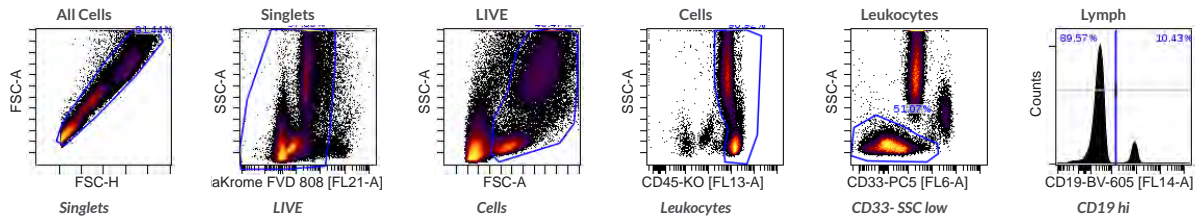


Figure 4. Gating hierarchy of B cells population.

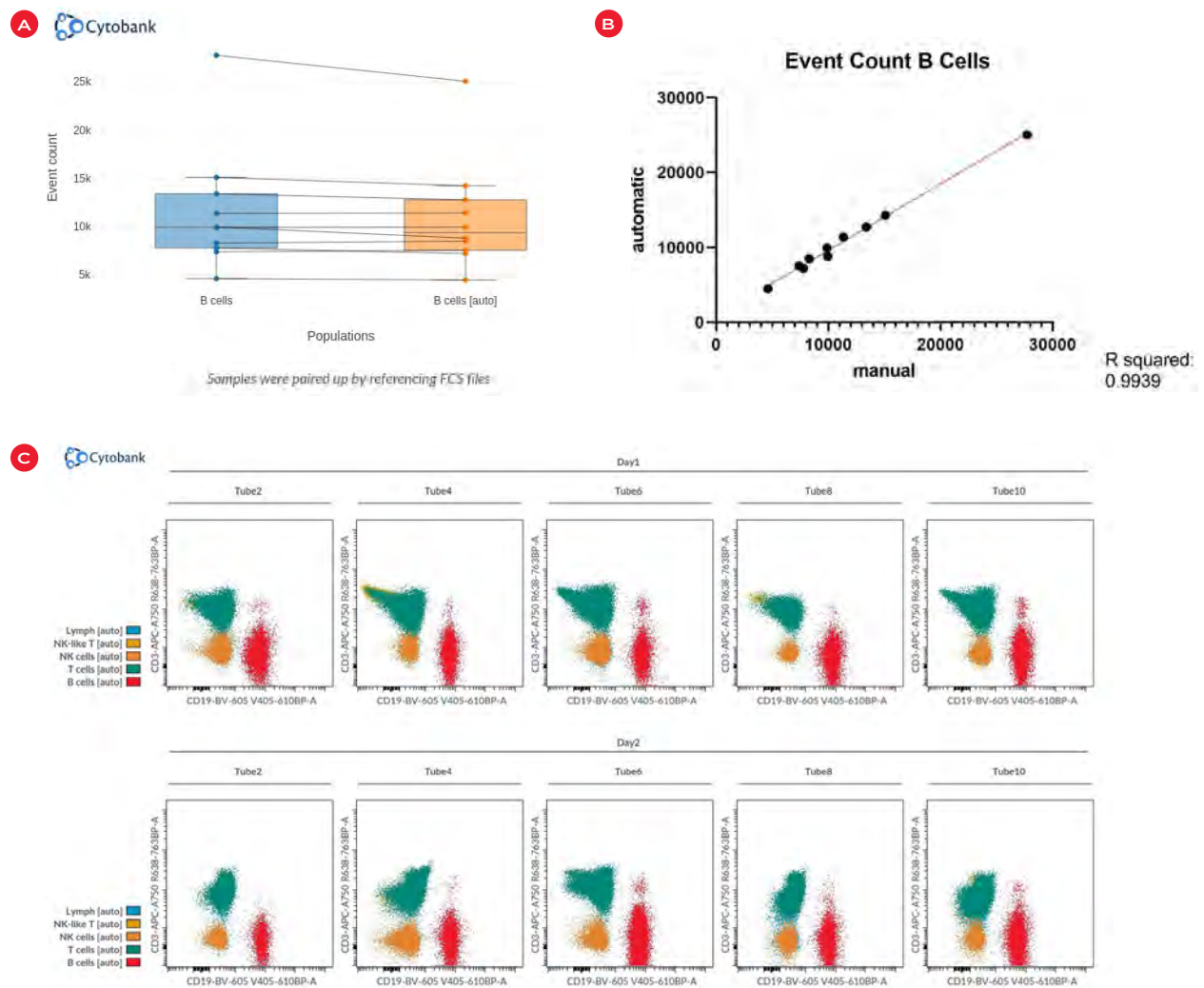


Figure 5. (A) Box plot comparing event count of manually and automatically gated Cells population. (B) Correlation of manual and automatic Cells population. (C) Dot plots for 5 exemplary samples with automatically identified Lymph and lymphocyte subset populations (NK-like T, NK cells, T cells, B cells) in the overlaid position.



## Intermediate monocytes: low-abundance population defined by modulated markers using quadrant gate

Intermediate monocytes were identified as a subset of the monocyte population based on their expression of CD45, CD33, HLA-DR, CD16 and CD14.

### intermediate

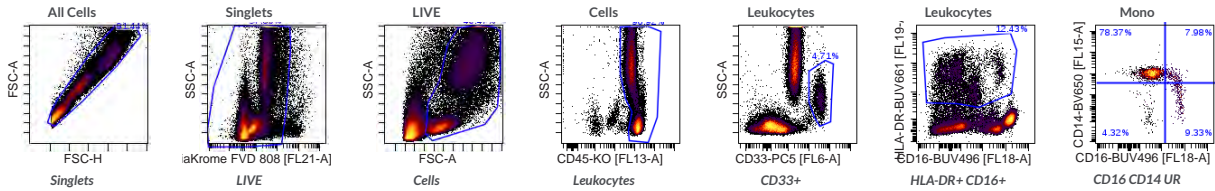


Figure 6. Gating hierarchy of intermediate monocyte population.

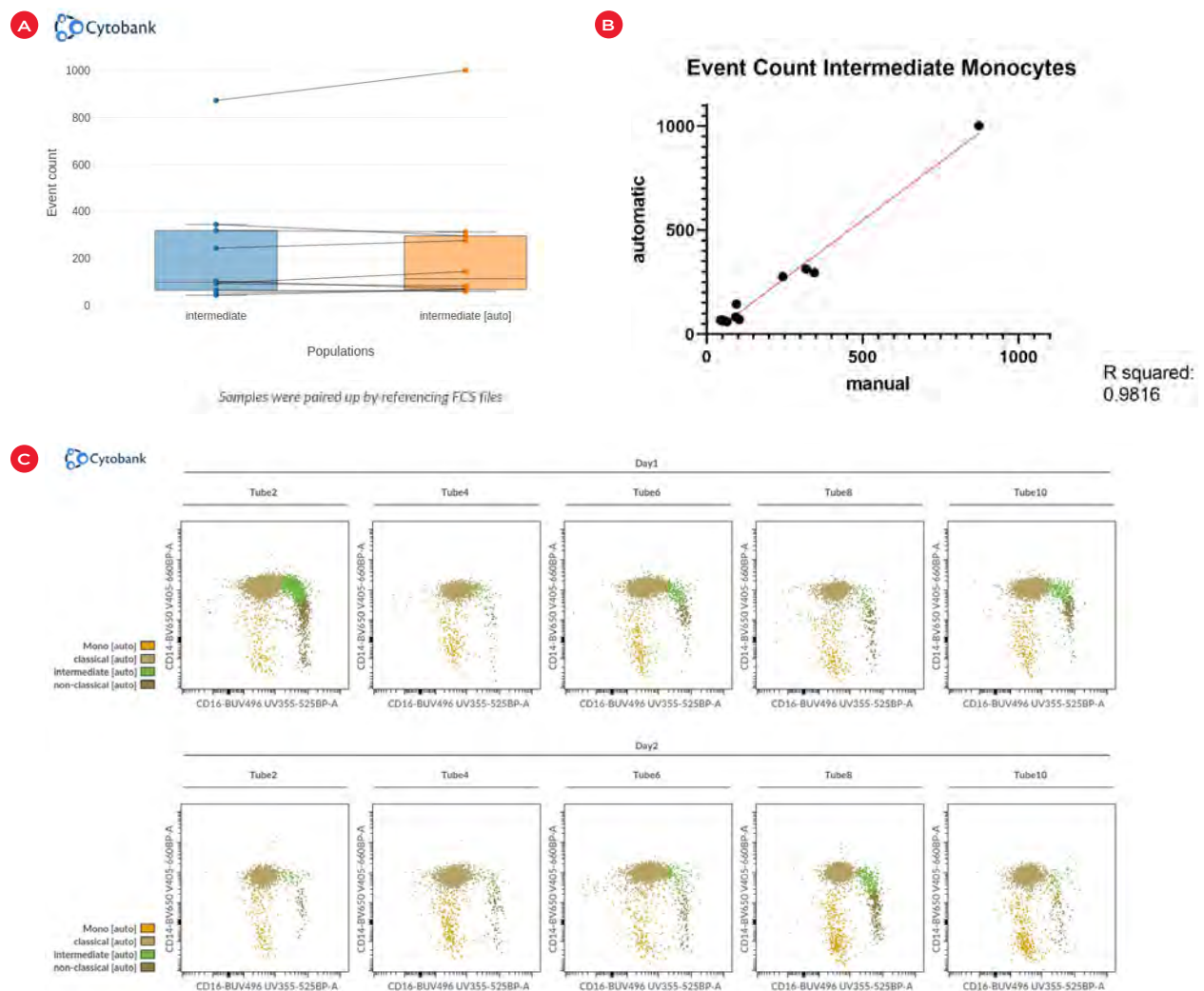


Figure 7. (A) Box plot comparing event count of manually and automatically gated intermediate monocyte population. (B) Correlation of manual and automatic intermediate monocyte population. (C) Dot plots for 5 exemplary samples with automatically identified monocytes and monocyte subset populations (classical, intermediate, non-classical) in the overlaid position.

## CD4+ CM T cells: distinct population defined using 11 gating steps

CD4+ central memory T cells (CM) were identified as CD45+, CD33-, CD19-, CD3+, CD56-, CD4+, CCR7+, CD45RA-, CD27+, CD28+, CD57-.

### CD4+ CM

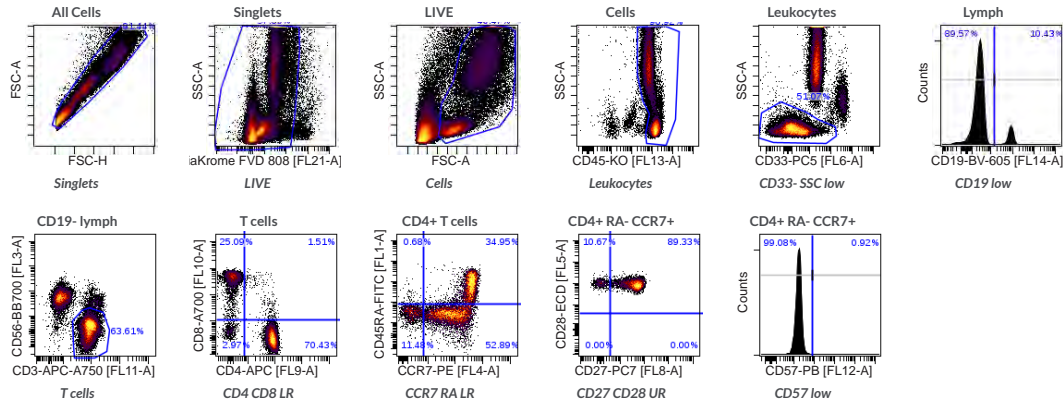


Figure 8. Gating hierarchy of CD4+ CM T cells population.

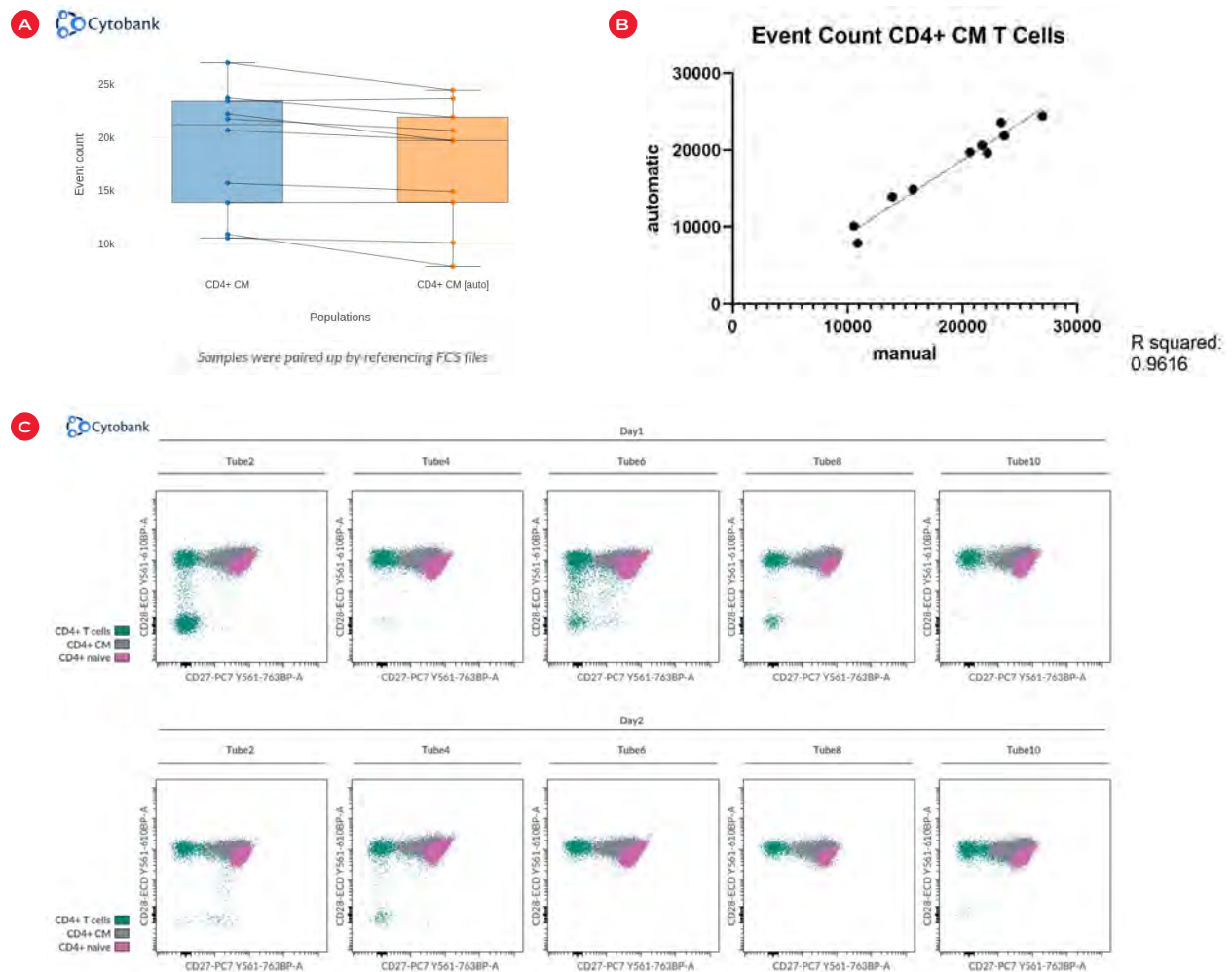


Figure 9. (A) Box plot comparing event count of manually and automatically gated CD4+ CM T cells population. (B) Correlation of manual and automatic CD4+ CM T cells population. (C) Dot plots for 5 exemplary samples with automatically identified CD4+ T cells and CD4+ CM and CD4+ naive subsets in the overlaid position.

## CD8+ TTM T-cells: rare population

CD8+ transitional memory T-cells (TTM) were identified as CD45+, CD33-, CD19-, CD3+, CD56-, CD8+ CD4-, CCR7-, CD45RA-, CD27+, CD28+, CD57+.

### CD8+ TTM

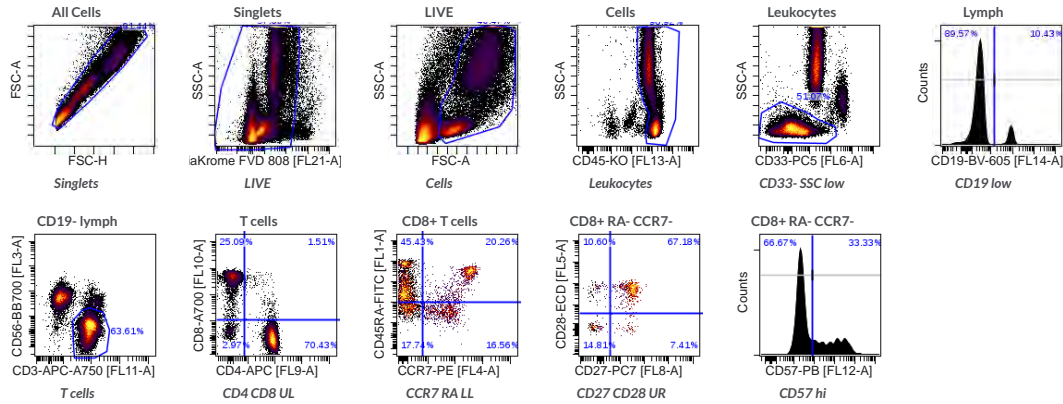


Figure 10. Gating hierarchy of CD8+ TTM population.

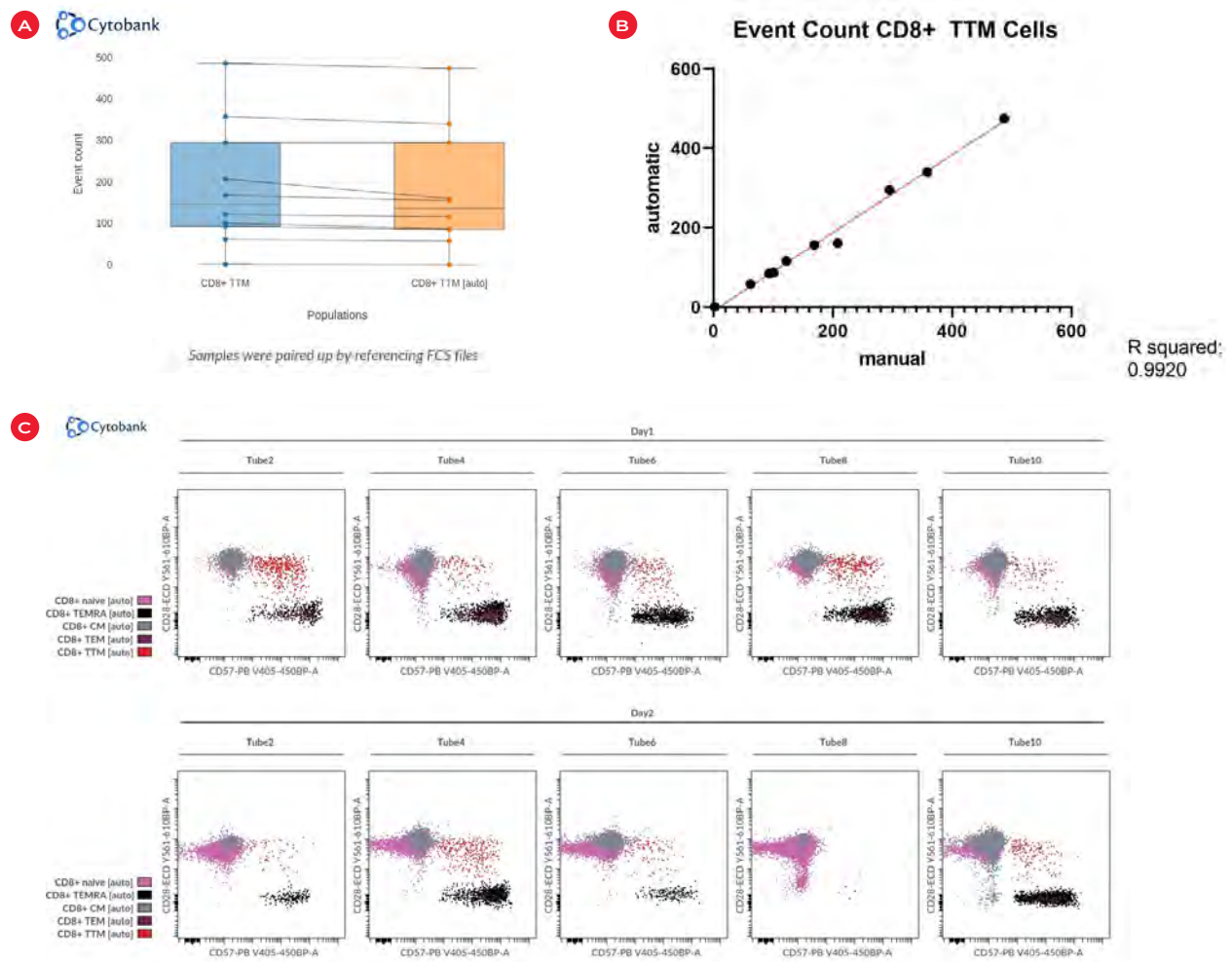


Figure 11. (A) Box plot comparing event count of manually and automatically gated CD8+ TTM cells population. (B) Correlation of manual and automatic CD8+ TTM population. (C) Dot plots for 5 exemplary samples with automatically identified CD8+ memory T cell subsets in the overlaid position.

For all evaluated populations, automatic results are comparable to manual gating and achieve an R squared value of well above 0.9.

### Automatic gating reduces hands-on time

In addition to reducing variability, automatic data analysis approaches reduce hands-on time. For both manual gating and Cytobank Automatic gating, a gating strategy and population hierarchy needs to be defined by the user. This way, prior knowledge is taken into account.

For Automatic gating, a subset of samples is then manually analyzed and a model is trained that can be applied to more samples. When using manual gating, all gates need to be reviewed for all samples and tailored by file.

For the Deep Immunophenotyping panel, the development of the gating strategy took 90 minutes. Analysis per file took on average of 7.5 minutes. As the Automatic gating model could be trained on 10 files and used to analyze the remaining 10 files, hands-on time was reduced by over 30%. Per analyzed sample, time required for gating and population identification was reduced by 50%.

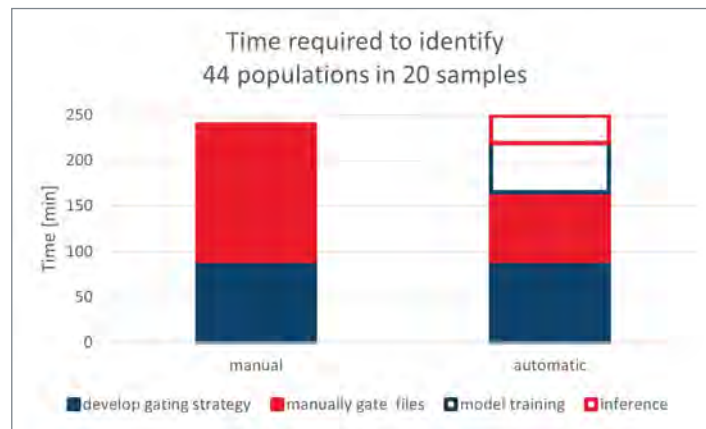


Figure 12. Time requirements for the identification of all populations in all 20 samples in the experiment.

### Automatic gating faithfully replicates manual population identification while reducing hands-on time for the analysis of a 19-color, 44-population-deep immunophenotyping assay

The automatic analysis of high-dimensional flow cytometry data requires some time investment to set up hypothesis-driven strategies for population identification. This initial time investment is balanced by a significant reduction in hands-on time for each additional sample that needs to be analyzed. In addition, it was shown that automatic gating can achieve performance comparable to an expert user. As automatic gating models can be shared among users on the Cytobank platform, automatic gating models have the potential to eliminate inter-operator variability.

The Cytobank platform, CytoFLEX LX, DURAClone IM T-cell Subsets dry reagent and ViaKrome 808 are For Research Use Only. Not for use in diagnostic procedures.

This protocol is for demonstration only, and is not validated by Beckman Coulter Life Sciences. Beckman Coulter Life Sciences makes no warranties of any kind whatsoever express or implied, with respect to this protocol, including but not limited to warranties of fitness for a particular purpose or merchantability or that the protocol is non-infringing. All warranties are expressly disclaimed. Your use of the method is solely at your own risk, without recourse to Beckman Coulter Life Sciences. Not intended or validated for use in the diagnosis of disease or other conditions.

© 2023 Beckman Coulter, Inc. All rights reserved. Beckman Coulter, the stylized logo, and the Beckman Coulter product and service marks used herein are trademarks or registered trademarks of Beckman Coulter, Inc. in the United States and other countries. All other trademarks are the property of their respective owners.

For Beckman Coulter's worldwide office locations and phone numbers, please visit Contact Us at [beckman.com](https://beckman.com)

2022-GBL-EN-100376-v2